Bulletin of Glaciological Research 23 (2006) *23–32*

Meteorological observation at July 1st Glacier in northwest China from 2002 to 2005

Akiko SAKAI[1], Yoshihiro MATSUDA[1], Koji FUJITA[1], Sumito MATOBA[2], Jun UETAKE[4], Kazuhide SATOW[5], Keqin DUAN[6], Jianchen PU[6], Masayoshi NAKAWO[7] and Tandong YAO[8]

1 Graduate School of Environmental Studies, Nagoya University, c/o HyRAC, Chikusa-ku, Nagoya 464–8601, Japan
2 Institute of Low Temperature Science, Hokkaido University, Sapporo 060–0819, Japan
4 Faculty of Bioscience and Biotechnology, Tokyo Institute of Technology, Ookayama, Meguro-ku, Tokyo 152–8551, Japan
5 Nagaoka National College of Technology, 888 Nishi-katakai-machi Nagaoak-city Niigata 940–8532, Japan
6 Cold and Arid Regions Environmental and Engineering Research Institute, Chinese Academy of Sciences, 260 Donggang West Road, Lanzhou 730000, China
7 Research Institute for Humanity and Nature, 335 Takashima-cho, Kamigyo-ku, Kyoto 602–0878, Japan
8 Institute of Tibet Plateau Research, Chinese Academy of Sciences, 100085, Beijing, China

(Received April 26, 2005; Revised manuscript accepted October 1, 2005)

Abstract

Meteorological observations were carried out at July 1st Glacier (J1G) in Northwest China. An automatic weather station was established at the glacier terminus 4295 m a.s.l. altitude from June 2002 to August 2005. Manual meteorological observations and dust particle counting have also been conducted at the Base Camp during the summers of 2002, 2003 and 2004. The catch ratio of the precipitation was calibrated, separating it into rain and snow depending on the air temperature, which relation has been observed at Base Camp. The calibrated annual precipitation in 2002 was about 340 mm, which was more than 20% above the observed value. Inter-annual variations in the meteorological data revealed that there were remarkable wet calm and cloudy periods during the summer 2002.

1. Introduction

Precipitation in mountain areas is relatively high in the arid region of northwest of China. In such areas, glaciers function as reservoirs of precipitation (Fountain and Tangborn, 1985). Water from the mountains has been an important resource in the downriver basin, oasis cities and desert. Therefore, fluctuation in the melt-water from glaciers should have some affect on human activity. Evidence of this can be found in ancient oasis cities in the desert that have fallen to ruin. Such environmental change would be caused by the change of water resources, which was caused by the reduction of discharge from mountain area.

Liu and Chen (2000) have revealed that the recent air temperature increase was larger at higher altitudes in the Tibetan Plateaus indicating that climate changes at high altitudes would be different from those in low altitude areas, where there is an abundance of prior meteorological data. Glaciological data were obtained beginning in the 1950s at the J1G in the Qilian Mountains of China. Moreover, glacial surveys have been carried out at several glaciers in the Qilian Mountains (Liu *et al.,* 1992). On the other hand, there is so far a dearth of long-term meteorological data such as covering more than one year at mountains higher than 4000 meters. Therefore, we set up an automatic weather station near the glacier, from which to collect meteorological data.

Precipitation is significant as an input water mass to the glacier basin area when we consider the discharge from the basin. The aim of this paper is to calibrate the observed precipitation, and to elucidate the current meteorological characteristics of the J1G.

2. Location and features of the glacier

J1G is located in the Qilian Mountains of northwest China (Fig. 1), 70 km south of Jiquan which is one of the oasis cities along the Western Corridor of the Yellow River. Figure 2 shows a topographical map of the J1G, which was produced by Shi (1988) in 1978. The glacier is located on the northern slope of the Qilian Mountains, and the top and terminal altitudes were about 5100 m a.s.l. and 4300 m a.s.l., respectively.

Sakai *et al.* (2004) have indicated that the shrinkage of J1G has become accelerated in recent 17 years. The glacier is of the polar type (Huang, 1990), and the instant ice temperature data has been quite low (−6℃

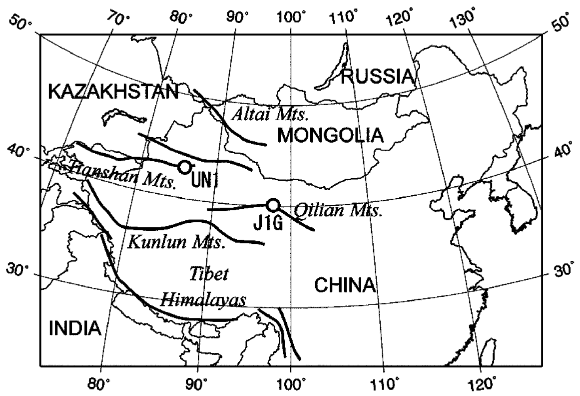

Fig. 1. Location of the July 1st Glacier (J1G) in the Qilian mountains, and the Urumqi No. 1 Glacier (UN1) in the Tian Shan mountains. Solid lines represent the mountain ranges. Thin lines indicate borderlines.

at 6 m depth in August in the 1970s) (Xie *et al.,* 1985). Therefore, some portion of the melt-water refreezes in the snow layer, making it necessary to take into account the refrozen amounts in order to estimate the mass balance of a glacier (Fujita *et al.,* 1996; Fujita *et al.,* 2000).

3. Observation

The Automatic Weather Station (AWS) started measurements near the glacier terminus from 10 June 2002 and continued collecting data until August 2005. Matsuda *et al.* (2004) reported preliminary meteorological data during the melting season in 2002. Data logging was carried out by CR-10x (Campbell Scientific, Ltd.). Instrument types, sampling intervals, logging intervals, and measurement heights of each element are summarized in Table 1. Unfortunately, the net radiometer was damaged in July 2004 and new one has set up in June 2005. Downward and upward long-wave radiations were also measured from September 10, 2003 beside the AWS site using infrared radiometers (MR-40, Eko, Co., Ltd.) at intervals of 10 minutes. Spectral response of the infrared radiometers was 3–50 μm.

Manual meteorological observations have also been carried out in the Base Camp at the altitude of 3668 m a.s.l. Observation periods and measured elements are summarized in Table 2. Air temperature was measured by an Assman psychrometer, and wind direction and speed have been measured by a aerovan produced by Nakaasa Co., Ltd. Precipitation was also measured at Base Camp using a tipping bucket with a logger (HoBo-event) whose resolution was 0.1 mm.

The vast Gobi Deserts lies to the north and the Taklamakan Desert to the west of the Qilian Mountains. Dust particles accumulating on the glacier surface blacken the surface and reduce the surface albedo. Therefore, dust particles were also counted at the Base Camp using a particle counter (KR-12, RION Co., Ltd.) and measured number with particles with 0.3, 0.5, 0.7, 1, 2 and 5 μm in diameter using 90° sideway light-scattering method. Those observations were carried out 1–5 times a day from June to September 2004.

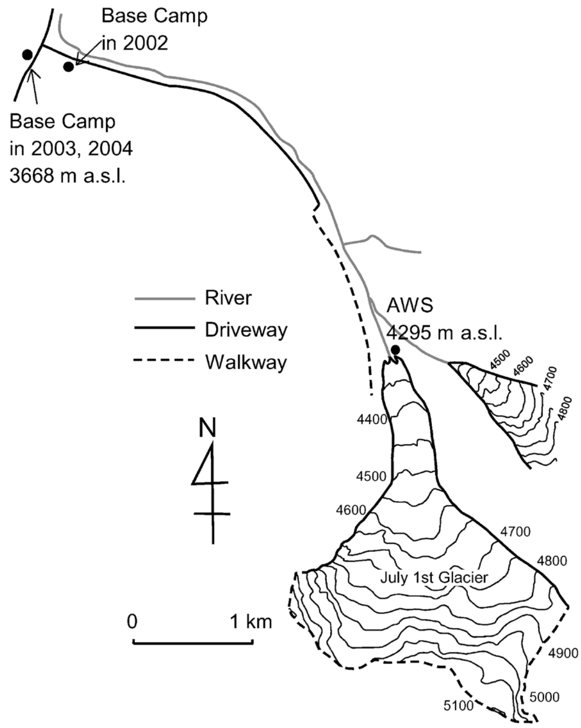

Fig. 2. Map of the J1G produced by Shi (1988) and locations of the Base Camp in Qilian mountains. 'AWS' indicates location of Automatic Meteorological Station.

4. Calibration of precipitation

Precipitation, which was a significant factor in evaluating the water balance of the glacier, was measured using a tipping-bucket rain gauge at the meteorological station near the terminus of the glacier. The gauge measurement for precipitation induces three different types of error, dynamic loss (caused by the deformation of the air flow field above the gauge orifice), wetting loss (caused by precipitation adhering to the inside wall of the gauge), and evaporation loss (caused by evaporation of the precipitation received by the gauge) (Sevruk, 1985). Dynamic loss is the most significant factor when considering snow measurement. The catch ratio of the precipitation by the tipping bucket rain gauge depends on the phase of the precipitation (rain or snow) and the wind speed (Yokoyama *et al.,* 2003). Thus, it is first necessary to investigate the occurrence of solid precipitation.

4.1. Occurrence probability of solid precipitation

The relation between the probability of the solid precipitation occurrence and air temperature is shown in the Fig. 3. Hail was excluded in the same figure

Table 1. Instrument name, company name, model type, sampling interval, logging interval, record type, measurement height for each item measured at Automatic Weather Station near the glacier terminus.

Item	Instrument	Manufactured by	Type	Sampling interval (sec)	Logging interval (mm)	Record type	Measurement height (cm)	Rermarks
Wind velocity	Anemometer	Young	Model 03001	3	10	Average	298	Threshold: $0.5\,ms^{-1}$
Wind direction	Vane	Young	Model 03101	3	10	Average	298	
Air temperature	Platinum resistance thermometer (Pt 100)	Vaisala	HMP45D	10	10	Average	184	
Relative humidity	Capacitance type humidity sensor	Vaisala	HMP45D	10	10	Average	184	
Downward solar radiation	Pyranometer	Eko Instrementa Co., Ltd.	MS-601	10	10	Average	221	Spectral response 0.3〜3μm
Upward solar radiation	Pyranometer	Eko Instruments Co., Ltd.	MS-601	10	10	Average	209	Spectral response 0.3〜 3μm
Scattered shortwave radiation	Pyranometer	Eko Instruments Co., Ltd.	MS-402	10	10	Average	207	
Net radiation*	Net radiometer	Radiation and energy Systems	Q7	10	10	Average	224	Spectral response 0.25〜60μm
Longwave radiation*	Pyranometer	Eko Instruments Co., Ltd.	MR-40	10	10	Average	200	Spectral response 3〜50μm
Ground temperature	Platinum resistance thermometer (Pt 100)	Hakusan Co. Ltd.	ST110	10	10	Average	0.5 cm depth	until July 2004
Precipitation	Tipping bucket rain gauge	Texas Electronics	TE525	10	10	Summation	80	0.1 mm per tip
Air pressure	Barometric pressure sensor	Vaisala	PTB210	10	10	Average		from Aug. 2003

*) Observation period June 2002〜July 2004

**) Observation period September 2003 〜August 2004

Table 2. Period and manual meteorological observation items at Base Camp. Circle indicates observed items.

		2002	2003	2004
Period	from to	9-Jun 1-Sep	18-Aug 10-Sep	25-Sep 10-Sep
Weather		○	○	○
Visibility		○		
Snow line altitude (m)		○		
Wind direction		○	○	○
Wind speed			○	○
Air temperature		○	○	○
Humidity		○	○	○
Surface condition		○		
Surface Temperature		○		
Sky radiation temperature		○		
Cloud amount		○	○	○
Cloud altitude (m)		○		
Particle counter for Dust measurement				○
Precipitation				○

since it was so rarely observed. The relation between air temperature and the percentage of solid precipitation occurrence is shown in the following equation.

$$P=-20.6T+147.8 \quad (2.3\leq T\leq 7.2). \qquad (1)$$
$$P=100 \quad (T<2.3)$$
$$P=0 \quad (T>7.2)$$

Where T is air temperature and P is the percentage of solid precipitation occurrence. The equation was derived from the data, when there were more than 3 precipitations. The temperature at 50% probability of solid precipitation occurrence was about 4.7℃ which is seen in Fig. 3. Ding and Kang (1985) reported a linear relation with the percentage of solid precipitation occurrence and air temperature at a meteorological station at Yanglonghe in the Qilian Mountains. Temperatures at 100%, 50% and 0% occurrence of solid precipitation were about 0, 3.6, and 7.2℃, respectively. Those temperatures are relatively lower than those in Fig. 3. Ageta and Higuchi (1984) have summarized the occurrence of solid precipitation in Asia. Ueno *et al.* (1994) reported that the air temperature at 50% occurrence of solid precipitation (: T_{50}) was 2.9℃ in the Tanggla Mountains of the Tibetan Plateau. Matsuo *et al.* (1981a, b) indicated that snow flakes tend to fall

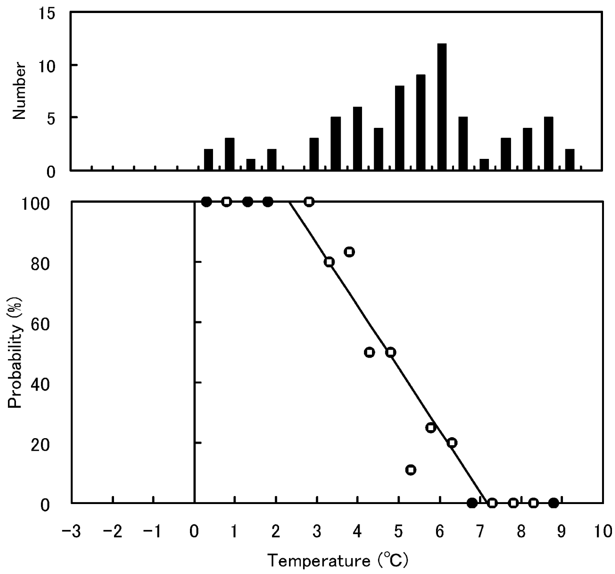

Fig. 3. Relation between the occurrence probability of solid precipitation and the air temperature (bottom), and number of precipitation events (above) at every 0.5℃ temperature interval. White circles indicate the occurrence probability of solid precipitation which occurred more than 3 times.

without melting in a low humidity atmosphere due to the relatively large evaporation of the snow flake. The T_{50} ranges were lower than that at the J1G, since the humidity was relatively high in those observed areas.

4.2 Calibration of precipitation for wind

Rain and snow were observed visually. Air temperature was also measured by the Assman psychrometer at a height of about 120 cm at the Base Camp (3668 m a.s.l.) during the precipitation period in August and September, 2003 and from June to August, 2004.

The catch ratio of the precipitation by the tipping bucket rain gauge depends on the precipitation type (rain or snow) and wind speed (Yokoyama *et al.,* 2003). Wind speed was measured at a height of 3 m (Matsuda *et al.,* 2004) at the meteorological station, while the height of the edge of the rain gauge was about 0.8 m. Wind velocity at the height z_i can be expressed as follows by the logarithmic law (Oke, 1987):

$$U_i = \frac{u_*}{\kappa} \ln\left(\frac{z_i}{z_0}\right), \tag{2}$$

where U_i (m sec^{-1}) is wind velocity at height z_i (m), κ is the Karman constant (=0.4), u_* is friction velocity (m sec^{-1}), and z_0 is roughness length. Since friction velocity is constant, the wind speed at the height of the rain gauge (height $z_{0.8}$) can be estimated by the following equation:

$$U_{0.8} = U_3 \frac{\ln\left(\frac{z_{0.8}}{z_0}\right)}{\ln\left(\frac{z_3}{z_0}\right)}, \tag{3}$$

where $U_{0.8}$ and U_3 are wind velocity at a height of 0.8 m and 3 m, respectively, and $z_{0.8}$ and z_3 are the respective heights of the rain gauge and anemometer at the meteorological station. Here, z_0 was assumed to be 0.01, which was applied to the soil surface (Oke, 1987). Precipitation can then be calibrated from the equation of Ohno *et al.* (1998),

$$CR = \frac{1}{1 + mU_{0.8}}, \tag{4}$$

where CR is the catch ratio of the rain gauge from 0 to 1, m=0.213 when the precipitation is snow, and m=0.0454 when the precipitation is rain according to Yokoyama *et al.* (2003). Yokoyama *et al.* (2003) established an equation to calibrate the observed precipitation data using a rain gauge 0.2 m in diameter, while we measured precipitation using a rain gauge 0.24 m in diameter. Actual precipitation at J1G, therefore, would be a slightly less than the calibrated precipitation since the catch ratio of the rain gauge with a larger diameter would be larger. Occurrence of solid precipitation was estimated from Eq. (3). Each calculation was carried out at intervals of 10 minutes. The measured data and calibrated value of precipitation, both snow and rain, are summarized in Table 3. Calibrated precipitation reached as much as 20% more than the amount of measured precipitation.

Figure 4(a) shows a 10-day summation of each snow and rain amount derived from the Eq. (3) from June 2002 to August 2005. The liquid precipitation (rain) appeared from July to early September. The total snow and rain amounts in each year from 15 June to 25 August, which corresponds to the summer season, are presented in Fig. 4(b), revealing that the ratio of rain amounts to total precipitation were relatively high during the summer of 2002, and the snow amount during the summer of 2005 was largest during the observed four years.

Unfortunately, no wind and air temperature data were measured automatically at the Base Camp. Precipitation observed at the Base Camp was calibrated using the wind speed measured at AWS. The temperature lapse rate used was −0.67℃ per 100 m height, which induced a temperature difference at AWS (measured by the AWS logger) and Base Camp (measured by Assman) from 10 Aug to 10 September, 2004.

Precipitation increases with altitude (Collins, 1989; Sevruk, 1994). The increasing rate is different at each site and season. Therefore, in order to evaluate the difference in precipitation at various altitudes, we observed the precipitation at Base Camp to be 3668 m a.s.l. altitude from May 26 to July 25, 2004, and com-

Table 3. Measured data and calibrated values of precipitation (PR), snow (SN) and rain (RA) were summarized in 2002, 2003, 2004 and 2005. Precipitation has increased about 20% by calibration.

Period		Observed data			Calibrated value			Increase by calibration PR%
from	to	PR mm (%)	SN mm (%)	RA mm (%)	PR mm (%)	SN mm (%)	RA mm (%)	
11-Jun-02	31-Dec-02	284 (100)	191 (67)	93 (33)	336 (100)	238 (71)	99 (29)	19
1-Jan-03	31-Dec-03	278 (100)	249 (90)	29 (10)	345 (100)	314 (91)	31 (9)	24
1-Jan-04	31-Dec-04	300 (100)	258 (85)	42 (15)	364 (100)	319 (86)	45 (14)	21
1-Jan-05	25-Aug-05	387 (100)	332 (86)	56 (14)	471 (100)	412 (86)	59 (13)	22

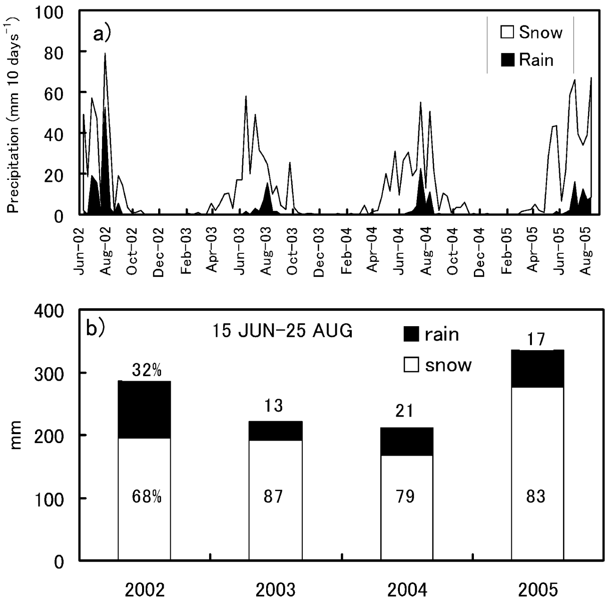

Fig. 4. (a): Fluctuation in 10 day-precipitation (rain and snow) from June 2002 to August 2005. (b): Total rain and snow from 15 June to 25 August in 2002, 2003, 2004, and 2005 respectively. Each number indicates the ratio of snow or rain to annual precipitation in%.

pared it with the precipitation measured at AWS near the glacier terminus.

The calibrated precipitations at AWS and BC from 28 May to 24 July, 2004 are shown in Fig. 5. The observed daily precipitation value at the Base Camp was often larger than that at AWS. This was because snow (solid precipitation) often fell at the AWS site (4295 m a.s.l.) when rain was falling at the Base Camp (3668 m a.s.l.). The tipping bucket rain gauge can measure instant falling liquid precipitation, while snow accumulating on the tipping bucket would be measured only after it had melted. This was why precipitation at the AWS was often observed after precipitation occurred.

Total precipitation at each station was 152 mm and 131 mm at AWS and Base Camp, respectively. Therefore, precipitation between the altitudes of 3668 and 4295 can be estimated from the meteorological station by assuming it increases proportionately with the altitude as shown by Ohta *et al.* (1994):

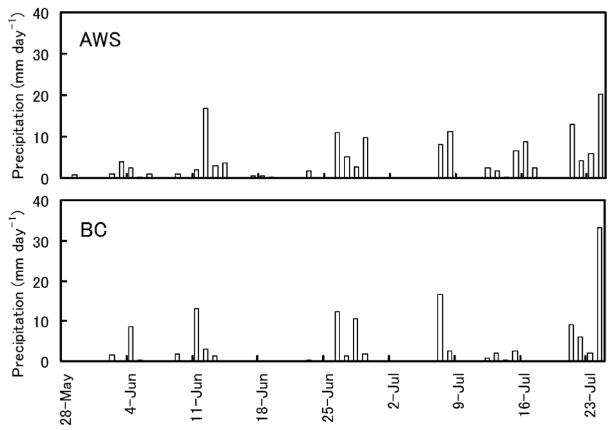

Fig. 5. Daily precipitation measured at Automatic Weather Station at 4295 m a.s.l. (above) and at the Base Camp at 3835 m a.s.l. (bottom).

$$P(h)=(1-c(4295-h))P_{aws} \quad (3668<h<4295), \quad (5)$$

where

$P(h)$ = Precipitation at the altitude h m a.s.l. (mm),
c = gradient of the precipitation to the altitude = 0.0002203 (constant number),

and

P_{aws} = Precipitation at AWS (mm).

Ohta *et al.* (1994) reported that the gradient of the precipitation to the altitude, c, was 0.00117 in the Tanggula Mountains, which was much larger than that at J 1G. It is necessary to observe meso-scale meteorological conditions when considering differences in the precipitation profile with altitude.

5. Result of observations

5.1 Meteorological data

Meteorological data in monthly averages, including the calibrated precipitation data, are summarized in Table 4.

Figure 6 the shows 15-day running mean of wind speed, air temperature, relative humidity, and downward solar radiation in each year (2002, 2003, 2004, and 2005). Monthly precipitation is also shown in Fig. 6. It is worth noting that there were remarkable time cy-

Table 4. Meteorological elements summarized as monthly averages. WS: Wind speed; TA: Air temperature; RH: Relative humidity; PR: Precipitation; TS: Soil surface temperature; AP: Air pressure; SD: Downward solar radiation; SU: Upward solar radiation; RN: Net radiation. 'AVE/SUM' shows the average values in 2003 for each item. Precipitation was summed. '—' indicates no data.

Year	Month	WS m sec^{-1}	TA ℃	RH %	PR mm	TS ℃	AP hPa	SD W m^{-2}	SU W m^{-2}	RN W m^{-2}
2002	Jun*	2.3	3.7	58	67.4	8.4	—	258	45	141
	Jul	1.9	5.0	71	110.3	10.2	—	199	28	114
	Aug	2.3	4.4	58	117.6	9.2	—	207	34	103
	Sep	1.7	−0.7	64	37.4	4.1	—	166	24	81
	Oct	2.9	−6.3	44	3.6	−3.7	—	147	29	38
	Nov	3.2	−11.7	33	0.0	−11.7	—	102	16	7
	Dec	3.1	−14.1	36	0.2	−15.4	—	72	15	−8
2003	Jan	2.9	−15.8	32	0.2	−17.4	—	88	17	−3
	Feb	3.0	−13.9	42	1.2	−13.8	—	118	37	17
	Mar	3.1	−11.6	42	2.9	−8.9	—	180	45	62
	Apr	3.4	−6.2	52	10.6	−2.3	—	221	59	93
	May	2.5	−2.7	57	39.7	2.7	—	244	51	125
	Jun	2.1	1.5	62	89.7	7.0	—	233	36	132
	Jul	2.3	3.4	66	113.4	8.0	—	226	32	135
	Aug	2.2	3.7	62	48.3	8.3	—	200	28	112
	Sep	2.3	0.1	52	32.2	4.6	607	208	34	96
	Oct	2.8	−5.8	41	6.0	−3.7	605	162	42	39
	Nov	3.6	−10.9	38	0.8	−10.7	600	93	23	5
	Dec	3.1	−15.7	32	0.0	−17.0	598	81	18	−7
AVE/SUM		2.8	−6.1	48	344.9	−3.6	—	171	35	67
2004	Jan	3.1	−17.3	39	0.4	−18.1	594	87	23	1
	Feb	3.3	−15.9	37	0.5	−14.9	596	129	25	32
	Mar	4.4	−10.8	43	4.7	−8.8	598	178	43	68
	Apr	2.8	−4.3	37	12.5	1.7	602	265	47	128
	May	2.4	−3.3	56	62.7	1.4	604	268	92	107
	Jun	2.4	1.0	59	66.5	6.7	605	246	43	138
	Jul	2.3	4.1	61	97.0	9.0	606	228	33	132
	Aug	2.2	3.7	65	83.6	8.0	606	212	31	—
	Sep	2.6	−1.1	53	21.3	3.0	607	192	249	—
	Oct	2.3	−6.7	45	13.7	−3.2	605	155	245	—
	Nov	3.2	−13.0	39	1.0	−12.9	602	99	267	—
	Dec	3.4	−14.2	38	0.5	−15.3	597	74	121	—
AVE/SUM		2.9	−6.5	48	364	−3.6	602	178	102	—
2005	Jan	3.3	−15.6	34	0.4	−16.1	594	87	130	—
	Feb	3.7	−14.8	32	0.0	−13.6	593	131	178	—
	Mar	2.9	−11.4	52	6.1	−8.1	599	190	366	—
	Apr	3.2	−7.1	41	7.6	−2.0	602	257	405	—
	May	2.7	−2.3	55	92.0	2.4	602	277	801	—
	Jun	2.6	1.8	59	82.4	6.6	605	270	355	—
	Jul	1.8	4.3	73	166.7	7.6	607	208	33	117
	Aug**	1.9	4.0	69	115.6	7.7	606	208	31	111

*: Period from 11 to 30 Jun., 2002
**: Period from 1 to 25 Aug., 2005

cles of a few weeks of wind speed, humidity, and solar radiation, and some wet weather and dry weather would also have been repeated at intervals of about 2 or 3 weeks from July to September in 2002.

Calibrated annual precipitation reached more than 300 mm, which corresponds to the results of Yang *et al.* (1992) and Zhu and Wang (1996). However, we could not calibrate the precipitation, which accumulated over the tipping bucket and was blown away by strong wind before flowing into the bucket. It will thus be necessary to calibrate it using a snow-depth sensor during winter rather than in the melting sea-

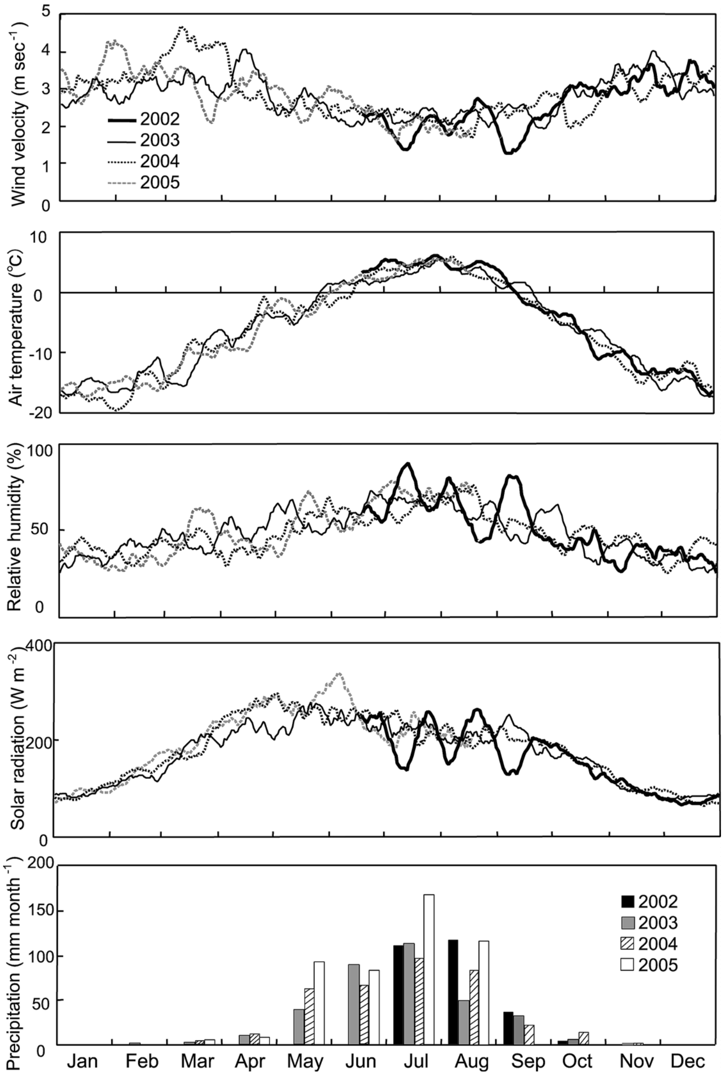

Fig. 6. 15-day running means of wind velocity, air temperature, relative humidity, and solar radiation in each year. Lowest box depicts monthly precipitation over three years.

son.

5.2 *Longwave radiation*

Figure 7(a) shows the observed daily mean downward and upward longwave radiations. The latter radiation (LU) can be calculated as follows using the ground surface temperature (T_s (K)) measured at the AWS site:

$$LU = \varepsilon\sigma T_s^4, \tag{6}$$

where σ is the Stefan-Boltzmann constant ($=5.67 \times 10^{-8}$ W m^{-2} · K^{-4}) and ε is the emissivity of the ground surface, which depends on the surface conditions, such as snow or debris. During the summer (no snow cover), the longwave radiation induced from the ground temperature measured by thermometer at AWS (Table 1) should be equal to the upward longwave radiation measured using the infrared radiometer (LU) by assuming that the ground surface around the AWS was homogeneous. ε can then be evaluated from the observed upward longwave radiation as follows:

$$\varepsilon = LU/\sigma T_s^4. \tag{7}$$

The average upward longwave radiation observed at the AWS and the surface temperature were 361.6 W m^{-2} and 282.5 K (9.4℃), respectively, from June to August, 2004. Therefore, the average ε was 1.00 with a standard deviation of 0.03 (at 10-minute intervals) suggesting that the ground surface at the site where upward longwave radiation was measured can be regarded as a black body.

Net radiation (RN) can be calculated from the measured upward (SU) and downward (SD) shortwave radiations and upward (LU) and downward (LD) longwave radiations as follows:

$$RN = SD - SU + LD - LU. \tag{8}$$

The observed net radiation using a net radiometer at

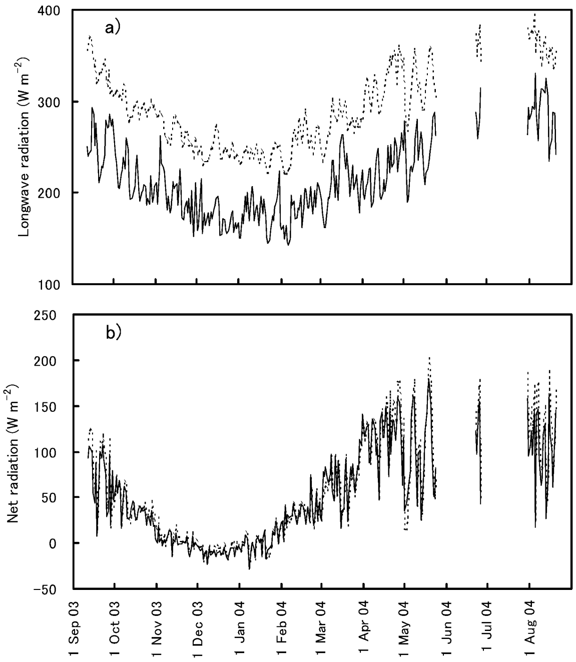

Fig. 7. (a): Observed daily mean downward (solid lines) and upward (dotted lines) longwave radiation. (b): Daily averages observed (dotted lines) and calculated (solid lines) net radiation.

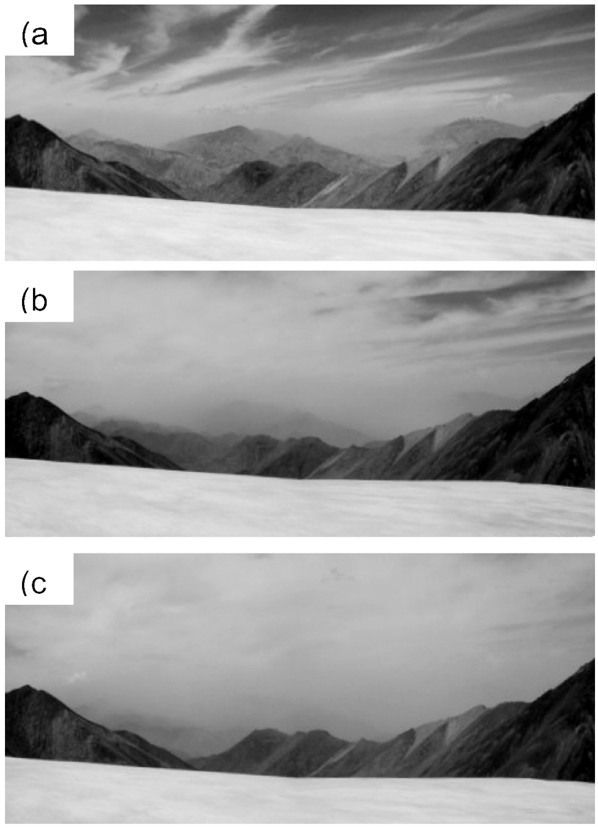

Fig. 9. Photographs showing time series of dust smog taken from 4800 m altitude facing north at the J1G. Photographs (a), (b) and (c) were shot at 12:06, 13:50 and 14:15, respectively, on 20 July 2004.

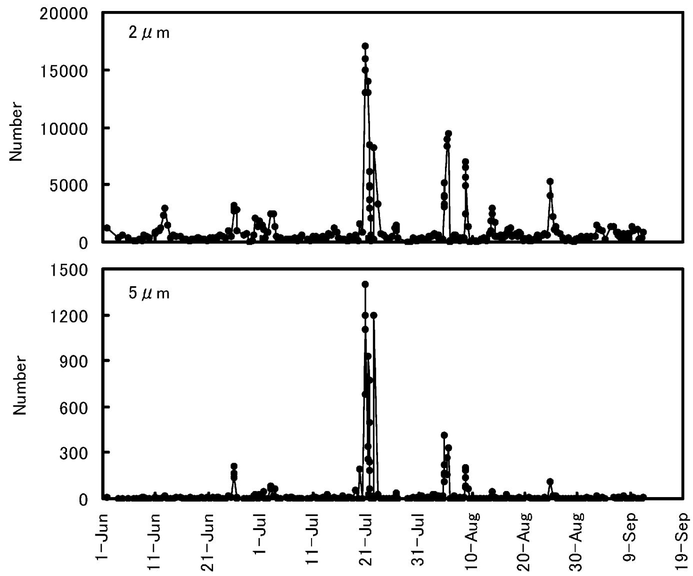

Fig. 8. Variations in number of dust particles 2μm (upper) and 5μm (lower) in diameter measured by a particle counter, 1–5 times a day.

AWS (*RNa*) was compared with the net radiation that was observed to induce observed downward and upward shortwave radiations and downward and upward longwave radiations using Eq. (8) (*RNc*) in daily average (Fig. 7(b)). The average difference between *RNa* and *RNc* was 4.5 W m^{-2}, with the standard deviation of 25.5 W m^{-2}. The discrepancy between *RNa* and *RNc* would be due to the measurement errors, the difference of spectral response of radiometers, and the inhomogeneity of the ground surface around the

AWS.

5.3 Dust particles

Fluctuations of the dust particle numbers 2 and 5 μm in diameter observed at Base Camp from June to August in 2004 were shown in Fig. 8. During the observation period there were several dust peaks indicating that dust storms had occurred. A large dust smog event occurred on 20 July 2004. Dust smog pictures were taken from the upper part of the glacier (at the altitude of 4800 m) facing north on 20 July (Fig. 9). First, the visibility was high, mountains could be seen well (Fig. 9a), the dust smog gradually increased and finally the visibility became less than 100 m (Fig. 9b, c). Dust smog then continued until the inception of heavy rain on 15:00 22 July. Dust particles were completely washed away by the heavy rains.

6. Concluding remarks

Precipitation is the most important factor when to considering the water balance at a basin. The catch ratio of the precipitation measured by a tipping bucket has been calibrated to the wind effect so as to distinguishing from solid and liquid phases determined from air temperature data. Calibrated annual precipitation in 2003 was about 340 mm, which was larger than about 20% of the measured precipitation.

Climatic features during the summer of 2002 were different from those of 2003, 2004 and 2005. In 2002, precipitation was relatively high, and the rain ratio in the precipitation was also high because of the relatively high air temperature. There were also several periods when it was relatively wet and calm with low solar radiation due to cloud cover. On the other hand, relatively dry, windy, fine (without cloud cover) days predominated in 2003 and 2004. It might be interesting to compare the meteorological data observed at the J 1G with those at cities near the observation site. Furthermore, the heat-balance elements for melting glacier ice during the summer 2002 might have differed from those in 2003, 2004 and 2005.

Acknowledgments

We would like to express our thanks to Prof. Yutaka Ageta of the Institute for Hydrospheric-Atmospheric Sciences, Nagoya University, for his valuable suggestions on these analyses. We also wish to thank all members of the Project for their valuable support in the field. The field research and data analyses were funded by a Grant-in-Aid for Scientific Research (Project No. 14209020) from the Ministry of Education, Culture, Sports, Science and Technology of Japan, and The Sumitomo foundation. This paper is a contribution to the Oasis Project (Historical evolution of adaptability in an oasis region to water resource changes), promoted by the Research Institute for Humanity and Nature (RIHN).

References

Ageta, Y. and Higuchi, K. (1984): Estimation of mass balance components of a summer-accumulation type glacier in the Nepal Himalaya. Geografiska Annaler, **66A** (3), 249–255.

Collins, D. (1989): Hydrometeorological conditions, mass balance and runoff from alpine glaciers. J. Oerlemans (ed.) *Glacier Fluctuations and Climatic Change.* Klüwer Academic Publishers, 235–260.

Ding, L. and Kang, X. (1985): Climatic conditions for the development of glacier and their effect on the characterictics of glaciers in Qilian mountains. Memoirs of Lanzhou Institute of Glaciology and Cryopedology, Chinese Academy of Sciences, **No. 5**, 9–15. (in Chinese)

Fountain, A. G. and Tangborn, A. (1985): The effect of glaciers on streamflow variations. Water Resources Research, **21**, 579–586.

Fujita, K., K. Seko, Y. Ageta, J. Pu and T. Yao. (1996): Superimposed ice in glacier mass balance on the Tibetan Plateau. J. Glaciol. **42** (142), 454–460.

Fujita, K. and Y. Ageta. (2000): Effect of summer accumulation on glacier mass balance on the Tibetan Plateau revealed by mass-balance model. J. Glaciol. **46** (153), 244–252.

Huang, M. (1990): On the temperature distribution of glaciers on China. J. Glaciol., **36** (123), 210–215.

Liu, X. and Chen, B. (2000): Climatic warming in the Tibetan Plateau during recent decades. International Journal of Climatology, **20**, 1729–1742.

Liu, C., Song, G. and Jin, M. (1992): Recent change and trend prediction of glaciers in Qilian Mountain. Memoirs of Lanzhou Institute of Glaciology and Geocryology, Chinese Academy of Sciences, **No. 7**, 1–9. (in Chinese)

Matsuda, Y., Sakai, A., Fujita, K., Nakawo, M., Duan, K., Pu J. and Yao, T. (2004): Glaciological observations on July 1st glacier in Qilian Mountains of west China during summer 2002. Bulletin of Glaciological Research, **21**, 31–36.

Matsuo, T. and Sasyo, Y. (1981a): Non-melting phenomena of snowflakes observed in subsaturated air bellow freezing level. Journal of Meteorological Society of Japan, **59** (1), 26–32.

Matsuo, T., Sasyo, Y. and Sato, Y. (1981b): Relationship between types of precipitation on the ground and surface meteorological elements. Journal of Meteorological Society of Japan, **59** (4), 462–472.

Ohno, H., Yokoyama, K., Kominami, Y., Inoue, S. and Takami, S. (1998): Catch ratios of gauges for solid precipitation in Hokuriku region. Seppyo, **60** (3), 225–231.

Ohta, T., Yabuki, H., Kioke, T., Ohata, T., Koike, M. and Zhang, Y. (1994): Hydrological observations in the Tanggula Mountains, the Tibetan Plateau—discharge, soil moisture and ground temperature—. Bulletin of Glacier Research, **12**, 49–56.

Oke, T. R. (1987): *Boundary Layer Meteorology.* Second edition. Methuen, London and New York pp. 435.

Sakai, A., Fujita, K. Matsuda, Y., Kubota, J., Duan, K., Pu, J., Nakawo, M. and Yao, T. (2004): Five decades of shrinkage of the July 1st Glacier in the Qilian Mountains of China. The 4th International Symposium on the Tibetan Plateau, Lhasa, China.

Sevruk, B. (1985): Summary report. Correction of Precipitation Measurements, Swiss Federal Institute of Technology, Zurich, 13–23.

Sevruk, B. (1994): Spatial and temporal inhomogeneity of global precipitation data. Desbois and Desalmand (ed.) *Global Precipitation and Climate Change.* NATO ASI Series Vol. **126**. 219–230.

Shi, Y. (1988): *An Introduction to the Glaciers in China.* Lanzhou Institute of Glaciology and Geocryology, Chinese Academy of Science Press. pp. 243.

Ueno, K., Endoh, N., Ohata, T., Yabuki, H., Koike, M., Ohta, T.

and Zhang, Y. (1994): Characteristices of precipitation distribution in Tanggula, Monsoon, 1993. Bulletin of Glacier Research, **12**, 39–46.

Xie, Z., Wu, G., Wang, L. and Wang, Z. (1985): Ice formation of glaciers in Qilian mountains. Memoirs of Lanzhou Institute of Glaciology and Cryopedology, Chinese Academy of Sciences, **No. 5**, 27–40. (in Chinese)

Yang, Z., Cao, Z. and Wang, Q. (1992): The distribution characteristics on space and time of precipitation of Heihe Basin in Qilian mountain. Memoirs of Lanzhou Institute of Glaciology and Geocryology Chinese Academy of Sciences, **No. 7**, 121–132.

Yokoyama, K., Ohno, H. Kominami, Y. Inoue, S. and Kawakata, T. (2003): Performance of Japanese precipitation gauges in winter. Seppyo **65** (3), 317–321. (in Japanese)

Zhu, S. and Wang, Q. (1996): Temporal-spatial distributions and recent changes of precipitation in the northern slopes of the Qilian Mountains. Journal of Glaciology and Geocryology. Vol. **18**, Special Issue, 296–304.